Remote Detection of Bioparticles in the THz Region

E. R. Brown[1], D.L. Woolard[2], A. C. Samuels[3], T. Globus[4], and B. Gelmont[4]

[1]University of California at Los Angeles, Los Angeles, CA, [2]Army Research Laboratory, Research Triangle Park, NC, [3]Edgewood Chemical and Biological Center, Aberdeen Proving Ground, MD
[4]University of Virginia, Charlottesville, VA

Abstract — **Recent measurements of the electromagnetic transmission through *Bacillus subtillus*, an innocuous anthrax substitute, have revealed absorption resonances in the THz region. A system-level analysis is carried out to show that at least one of the resonances (centered at 14.05 cm^{-1} , or 421 GHz) is located at a frequency of low enough atmospheric absorption to be detectable by an active remote sensor – a differential absorption radar.**

I. INTRODUCTION AND SUMMARY

Through pioneering research conducted at Purdue Univ., U. Virginia, and the U.S. Army, it has been shown that biomolecules can display strong absorptive resonances in the THz region of the electromagnetic spectrum. A good example is the torsional modes in DNA or a helical protein. Subsequent experiments on bioparticles, such as *bacillus (B.) subtillus* spores, have shown strong attenuation resonances that are thought to be associated with the protein cladding of the spore. Five resonances were observed (see Table I) that are repeatable and strong enough that one can estimate their detectability in a remote sensor.

This paper summarizes a study of the remote detection of *B .subtillus* by three sensor modalities: (1) passive incoherent (i.e., direct detection), (2) passive coherent (i.e., heterodyne radiometry), and (3) active incoherent (i.e., differential absorption radar). The passive techniques are the standard at THz frequencies because of their simplicity and lack of dependence on powerful coherent sources, which become more and more scarce and expensive with increasing frequency. They can also achieve high sensitivity if cryogenic electronics, such as superconducting bolometers or tunnel junctions, are used in the receiver front-end. However because of the small absorption cross section of the typical bioparticle resonance and the strong absorption by water vapor in the THz region, the passive techniques in the present study were found to be too insensitive at the ranges (up to 1 km) and the bioparticulate concentrations ($<<10^5$ cm^{-3}) relevant to biowarfare defense and related applications. And this ignores the deleterious effects of atmospheric and background (i.e., sky temperature) fluctuations.

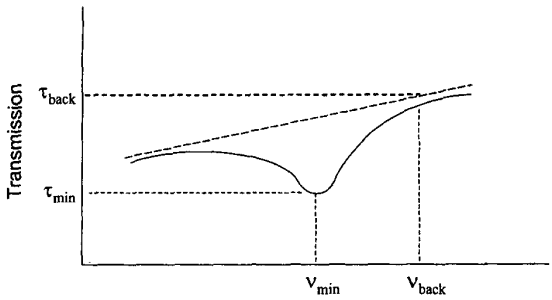

Fig. 1. Notional bioparticle absorption signature

Active sensors are potentially more sensitive than passive ones since they provide their own source of coherent radiation at a spectral density far above the background levels. A promising active architecture is the differential-absorption radar with a coherent transmitter operating minimally at two frequencies – one at the center of the absorption signature and one at the edge. By subtracting the received power alternately at the two frequencies, the absorption signature can be detected even in the presence of fluctuations in the atmosphere caused by wind and variable humidity. The technique is similar in principle to differential absorption lidar (DIAL) commonly used at IR wavelengths.

II. ABSORPTION SIGNATURE CHARACTERISTICS

A representative absorption signature is shown in Fig. 1 as it would appear in the power transmitted through a cloud of bioparticles. The background transmission in the THz region generally has a complex behavior. Although shown in Fig. 1 as a slowly increasing transmission with frequency, the background could display the opposite slope or be resonant depending on the proximity to water absorption lines. In any case the bioparticle absorption introduces a broad "dip" in the transmission spectrum that is characterized by a minimum τ_{min} at frequency ν_{min} , a depth $\Delta\tau$, and a half-width $\Delta\nu$. We take $\Delta\tau$ as the absolute difference between τ_{min} and the background transmission τ_{back} measured at a frequency ν_{back} on

0-7803-7239-5/02/$10.00 © 2002 IEEE

Table I. THz absorption signatures of *B. Subtillus*			
Freq, ν_{min}	α_0 (ν_{min}) (cm^{-1})	ν_{back} , $\Delta\nu$ (GHz)	τ (ν_{back})
327 GHz	1.3	334.5, 7.5	0.008
421.5 GHz	0.7	430.5, 10.0	0.25
619.5 GHz	1.3	600.0, 19.5	$\sim 10^{-11}$
940.05 GHz	1.7	930.0, 10.05	$\sim 5 \times 10^{-4}$
1075.5 GHz	1.2	1057.5, 18.0	$<10^{-30}$

whichever side of ν_{min} that τ is greater (e.g., in Fig. 1 $\nu_{back} >> \nu_{min}$). Hence $\Delta\nu \equiv |\nu_{min} - \nu_{back}|$. And if we assume that the concentration of bioparticles, ρ, is low enough that their attenuation can be described by a coefficient α that is linearly dependent on ρ and that affects the transmission through the Lambert-Beer law $\tau(\nu) = \exp[-\alpha_0(\nu)L\rho/\rho_0]$. In this expression L is the thickness of the bioparticle cloud and α_0 is a reference attenuation coefficient measured at a concentration ρ_0 that may be much different than the actual ρ. For the signature of Fig. 1 and assuming that the background transmission at each ν is constant, we have

$$\Delta\tau \equiv \tau_{back}\{1 - \exp[-\alpha_0(\nu_{min})L\rho/\rho_0]\} \qquad (1)$$

Listed in Table I are the values of ν_{min} , $\alpha_0(\nu_{min})$, ν_{back} and $\Delta\nu$ derived from laboratory transmission measurements through dry films of *B. subtillus* containing $\rho_0 \approx 1 \times 10^{12}$ cm^{-3} – a density that is necessary to get an accurate measure of $\Delta\alpha$, but is much larger than expected in airborne bio-warfare agents. The results listed in Table I describe five different absorption features having center frequencies between 327 and 1075 GHz. In the THz region, the remote detection of these signatures depends critically on the atmospheric transmission $\tau(\nu_{back})$.

III. Sensor-Target Scenario

The remote detection of bioparticles also depends critically on the scenario, which means the relative orientation of sensor and target, the physical size of the target, the optical depth of the absorbing species in the target, the atmospheric transmission between sensor and target, the background radiation, etc. For simplicity this analysis adopted the simple scenario shown in Fig. 2 consisting of a ground- or air-based active sensor looking into the sky at a target consisting of a cloud of dry bioparticles at temperature T_M and pressure P. The cloud is assumed to have physical thickness L and to be located at a range R from the sensor. Behind the cloud is a

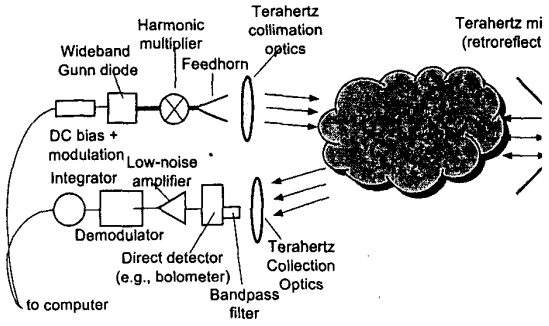

Fig. 2. Block diagram of sensor scenario and proposed differential absorption spectrometer.

retrodirective mirror that allows the transmitter and receiver to be co-located. The mirror is oriented relative to the sensor along a line that cuts through the thickest part of the cloud. The transmitter is assumed to radiate a constant power sequentially at the two frequencies ν_{min} or ν_{back} , defined in the previous section.

IV. Atmospheric Transmission

Because the THz region is notorious for high atmospheric attenuation from indigenous molecules, it is essential to estimate the transmission τ_{back} as part of the sensitivity analysis. We have applied a commercial radiative transport code, PCLnWin [1] which is based on the Fascode engine originally developed by the U.S. Air Force. The code solves for the radiation transmission as a function of slant angle and range for different model atmospheres in the presence of the common molecular species. Each absorption line is represented by the Voigt model with kinetic coefficients that account for pressure and Doppler broadening and that are fed into PcLnWin from the HITRAN96 database. The predominant absorber in the THz region is water vapor, which is better known for its lines at 22 and 183 GHz - the former having impacted radar history and the latter being the basis for atmospheric sounding radiometers. Several of the water lines in the THz region above 300 GHz are much stronger than these two.

Fig. 3 shows the overall transmission spectrum computed by PcLnWin for a 1 km path at a slant angle of 5°, a relative humidity of 60%, and for the 7 atmospheric constitutents: H_2O, O_2, CO, CO_2, O_3, N_2O, and CH_4. Below 300 GHz the transmission is greater than 50% except at the strong water line and molecular oxygen band at 60 GHz. Above 300 GHz the water lines are so strong that with pressure broadening become opaque sub-bands through which atmospheric transmission is practically impossible. Fortunately, a few transmission windows

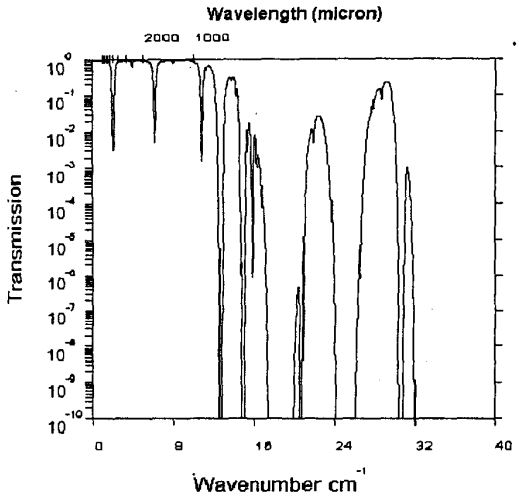

Fig. 3. Atmospheric transmission computed by PCLnWin (1 cm^{-1} = 30 GHz).

persist, such as the ones around 400, 670, and 840 GHz. In analyzing the detectability of bioparticles it is important to consider the proximity of their signatures to these opaque sub-bands and transmission windows.

Listed in Table I is the atmospheric transmission computed by PcLnWin for the 5 signatures of *B. Subtillus* at the line-center frequencies. Because of the high relative transmission ($\tau \approx 0.25$), the signature centered at 421 GHz has the best chance of being detected by an active remote sensor having practical levels of transmit power.

V. SENSOR SIMULATION

For the sensor architecture and scenario shown in Fig 2 and given the model of atmospheric propagation discussed above, the signal power at the receiver (Rx) can be estimated analytically given reasonable assumptions about the beam pattern of the transmitter (Tx). If we assume that the lateral extent of the beam is much smaller than the cloud at the range where the beam passes through, then the received power can be related to the transmitted power P_T by the following (Friis) transmission expression

$$P_R(\nu) = \frac{P_T G_T A_R}{4\pi R^2}\tau(\nu) \qquad (2)$$

where G_T is the gain of the Tx antenna, and A_R is the effective area of the Rx and R is the round-trip path length between. The R^{-2} dependence occurs in (2) instead of the usual R^{-4} radar factor because the retrodirective mirror is assumed to be perfectly specular. If we assume the Tx antenna is diffraction limited (easy to achieve in the THz region), then $G_T = 4\pi A_T/\lambda^2$, so that Eq. (2) can be written

$$P_R(\nu) = \frac{P_T A_T A_R \tau(\nu)}{R^2 \lambda^2} \qquad (3)$$

The Rx noise power will generally be the sum of two terms: (1) background electromagnetic noise caused by fluctuations in the received power, and (2) electrical noise caused by fluctuations of various physical quantities in the electronic devices of the Tx or Rx. In the THz region, the background power is associated with blackbody radiation coming from the sky, the bioparticle cloud itself, or the optics, all of which are assumed to be at or near an ambient temperature of 290 K. At this temperature and in the THz region $h\nu/k_BT \ll 1$ ($k_B \equiv$ Boltzman's constant), so the Planck distribution for the blackbody radiation can be approximated in the Rayleigh-Jeans limit. Furthermore, if the Tx is radiating only a single frequency at a given time, then its power should be contained within one spatial mode. The Rx would then be optimally designed to receive just this mode, so that the received background power would be,

$$P_B \approx (4h\nu k T_B B/\eta)^{1/2} \qquad (4)$$

where B is the RF bandwidth and η is the receiver coupling efficiency [2]. In a well-designed incoherent receiver, the electrical noise will be dominated by noise of the front-end direct detector. If we assign the detector a noise-equivalent power of NEP_{det}, the overall receiver NEP can be written,

$$NEP_{rec} \approx (4h\nu k T_B B/\eta + NEP_{det}^2)^{1/2} \qquad (5)$$

Given the above expressions for the signal and noise, we can estimate the power S/N ratio of a direct receiver in baseband by including the effect of integration,

$$\frac{S}{N} \approx \frac{P_R}{NEP_{rec}}(2t_{int})^{1/2} \qquad (6)$$

where t_{int} is the integration time. Substitution of (3) and (5) into (6) then yields

$$\frac{S}{N} \approx \frac{P_T A_T A_R \tau(\nu)}{R^2 \lambda^2} \frac{1}{(4h\nu k T_B B/\eta + NEP_{det}^2)^{1/2}}(2t_{int})^{1/2} \qquad (7)$$

To account for the change in Tx frequency that occurs in differential mode, we assume the Tx power remains constant and the duty cycle at each frequency is 50%. Hence the S/N is degraded by about a factor of two, and

Table II. Parameters used in sensor simulation	
Background temperature (K)	290
Detector coupling efficiency	0.5
Line center frequency (GHz)	421
Background frequency (GHz)	431
Linewidth (GHz)	10
Line center abs coeff (1/cm)	0.7
Background transmission	0.25
Spectral bandwidth (GHz)	10
Integration time (s)	1.0
Transmit power (mW)	1.0
Tx aperture (cm^2)	100
Rx aperture (cm^2)	100
Tx-Rx separation (m)	1000
Cloud thickness (cm)	variable
Cloud temperature (K)	290
Molecule density (cm^{-3})	$10,10^3,10^5$

$$\Delta P_R(\nu) = \frac{P_T A_T A_R \Delta\tau(\nu)}{R^2\lambda^2} \quad (8)$$

$$\left(\frac{S}{N}\right)_D \approx \frac{P_T A_T A_R \Delta\tau}{R^2\lambda^2} \frac{1}{(4h\nu kT_B B/\eta + NEP_{det}^2)^{1/2}} \left(\frac{t_{int}}{2}\right)^{1/2} \quad (9)$$

We have computed (9) for the sensor parameters listed in Table II and for three different concentrations of *B. subtillus*, ρ = 10, 10^3, and 10^5 cm^{-3}, which roughly span the interesting range for bio-warfare defense. The results are plotted vs cloud depth in Fig. 4 for a fixed Tx-to-Rx separation of 1.0 km (0.5 km sensor to mirror). In Fig. 4(a) the Rx detector is assumed to have NEP=$1x10^{-10}$ W-$Hz^{-1/2}$ corresponding to a state-of-the-art room-temperature bolometer (e.g., micro Golay cell). In Fig. 4(b) the Rx detector is assumed to have NEP = $1x10^{-13}$ W-$Hz^{-1/2}$ corresponding roughly to a state-of-the-art cryogenic (4.2 K) bolometer (e.g., silicon composite).

We have already used the results of Fig. 4 for quantifying higher-level system metrics such as the minimum detectable concentration MDC (i.e., concentration where S/N=1) and the probabilities of detection, Pd, and false alarm Pfa. For example, according to Fig. 4(b), in a cloud 20 m thick at a stand-off of 0.5 km, the MDC is 10^3 cm^{-3}. Assuming that all noise mechanisms in the Rx are statistically Gaussian and setting the signal threshold at 0.2 nW, we find Pd and Pfa values under these conditions to be approximately 0.4 and 0.1, respectively – unsatisfactory for most applications. However, the enhanced S/N at greater cloud depth in Fig. 4(b) allows for more reliable detection. For example, a cloud depth of 20 m and a concentration of 10^4 cm^{-3} yields a S/N of 10 and associated Pd and Pfa values of 0.75 and 0.006 if the threshold is increased to 0.9 nW.

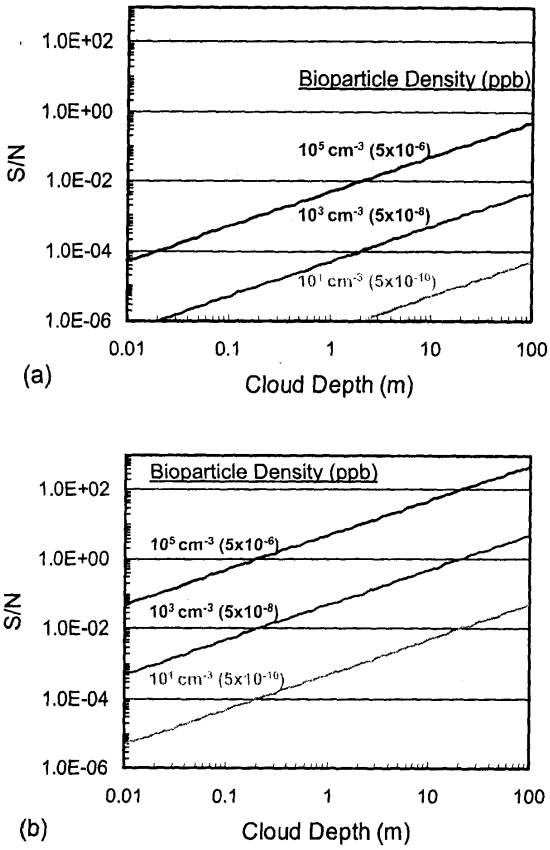

Fig. 4. S/N ratio as a function of bioparticle cloud depth for the parameters in Table II and direct detectors having (a) NEP = $1x10^{-10}$ $W/Hz^{1/2}$ and (b) NEP = $1x10^{-13}$ $W/Hz^{1/2}$.

VI. Conclusion

Although more rigorous calculations and experiments are needed, this paper establishes a first step toward the feasibility of detecting bioparticles, similar to anthrax spores, at a useful stand-off. The suggested sensor (a differential absorption radar) and the favored attenuation signature frequency (around 421 GHz) are both practical using commercially-available devices and components.

Acknowledgement

The first author acknowledges support from the U.S. Army Research Office Scientific Services Program.

References

[1] Ontar Corp., No. Andover, MA 01845-2000

[2] R.H. Kingston, "Detection of Optical and Infrared Radiation," (Springer, New York, 1978).